



Removal of Pb^{2+} , Ni^{2+} and Cd^{2+} ions in aqueous media using functionalized MWCNT wrapped polypyrrole nanocomposite

Rajakumar Kanthapazham^a, Chandramohan Ayyavu^b,
Dharmendirakumar Mahendiradas^{a,*}

^aDepartment of Applied Science and Technology, Anna University, Chennai 600 025, India, email: kumarkraja84@gmail.com (R. Kanthapazham), Tel. +91 4422359206; email: mdkumar@annauniv.edu (D. Mahendiradas)

^bMechanical Engineering Program, Texas A&M University at Qatar, Engineering Building, Education City, P.O. Box 23874, Doha, Qatar, email: acmohann@gmail.com

Received 2 February 2015; Accepted 4 August 2015

ABSTRACT

Functionalized multi-walled carbon nanotubes, a wrapped polypyrrole (PPy/o-MWCNT) nanocomposite, were prepared by in situ chemical oxidative polymerization. Characterization of the PPy/o-MWCNT nanocomposite was carried out using attenuated total reflectance infrared spectroscopy, Raman analysis, diffuse reflective ultraviolet–visible spectroscopy, powder X-ray diffraction, thermogravimetric analysis, scanning electron microscopy (SEM), energy dispersive analysis of X-rays (EDAX), transmission electron microscope (TEM) and selective area electron diffraction pattern (SAED). The obtained results confirmed successful synthesis of PPy/o-MWCNT nanocomposite. TEM provided the information about the wrapped tubular carbon nanotubes present in the polymer matrix and SAED pattern additionally confirms the crystalline pattern of the metal-loaded adsorbent. SEM images showed the o-MWCNT even dispersion of polymer matrix beyond the magnification of 200–500. EDAX data revealed the loading of metal ions onto polymer surface which was confirmed due to the presence of corresponding. The PPy/o-MWCNT nanocomposite was used as an efficient adsorbent for the removal of Pb^{2+} , Ni^{2+} and Cd^{2+} ions in aqueous media. Batch experiments show maximum adsorption capacity of PPy/o-MWCNT nanocomposite on Pb^{2+} (408 mg/g), Ni^{2+} (409 mg/g) and Cd^{2+} (392 mg/g). The heavy metal ions adsorption on PPy/o-MWCNT nanocomposite shows fast process and the kinetics followed a pseudo-second-order rate equation ($R^2 \approx 0.99$).

Keywords: MWCNT; Polypyrrole nanocomposite; Adsorption; Pb^{2+} , Ni^{2+} and Cd^{2+} ; Kinetic and thermodynamic studies

1. Introduction

Water is one of the prime elements that is responsible for life on earth. Elevated levels of heavy metal ions like lead, nickel, copper and cadmium in drinking

water are found to have deleterious effects on human health and natural environment. Due to the non-biodegradability and long biological half-life, heavy metal ions can be accumulated in the environmental elements such as food chain and thus may cause a significant danger to the human health [1–4]. The most

*Corresponding author.

common methods that have been used for the treatment of wastewater containing heavy metal ions include reduction/chemical precipitation, coagulation and flocculation, reverse osmosis, ion-exchange, ultra-filtration and adsorption [5]. Adsorption is an effective purification and separation technique used in industry for water and wastewater treatment [6]. The various adsorbents used to remove the heavy metal ions from aqueous media are activated carbon [7], peat moss [8], fly ash [9], biomaterials [10], zeolites [11], synthetic resins [12] and carbon nanotubes (CNTs) [13]. These adsorbents have poor recyclability and less long-life. So, there is a need for new adsorbent material which would be an effective alternative for metal ion adsorption from aqueous media.

CNTs have led research to new area in many interdisciplinary investigations, as the advantages of CNTs are unique in structural, electronic, optoelectronic, semiconductor, mechanical, and chemical and physical properties [14]. A multi-walled CNT is an effective adsorbent in the removal of heavy metal ions from aqueous media due to its high adsorption capacity and selectivity [15]. Functionalized multi-walled CNT is also considered to be fabricated easily available polymer adsorbent and environmentally stable. However, most of the available studies are conducted in the removal of heavy metals by the preformed multi-walled CNT [16].

Conducting polymers have potential application in various fields such as microelectronics, composite materials, optics and biosensors [17], and as adsorbent [18]. Conducting polymer nanocomposites have some distinctive properties such as easy preparation, cost effective, environmentally stable and unique doping mechanism. The presence of amine group in the conducting polymer has created attention, since it has an ability to bind transition metal ions, which have strong affinity towards divalent metal ions [19]. However, CNTs have specialized properties to make nanocomposite of effective aspect ratio, even dispersion in polypyrrole matrix and the interfacial adhesion between CNT additives and polypyrrole matrix. Good interfacial bonding is essential to ensure efficient charge transfer from the polypyrrole matrix to the functionalized CNTs lattice and it is one of the critical issues related to the functionality of CNT-polypyrrole nanocomposite. The functionalized MWCNT-wrapped polypyrrole nanocomposite adsorbent has been a cost-effective adsorbent and also it enhances the adsorption capacity and recoverability of heavy metal ions.

In the present study, the functionalized MWCNT-wrapped polypyrrole nanocomposite was synthesized and characterized by important instrumental techniques. Adsorption of bivalent metal ions (Pb^{2+} , Ni^{2+}

and Cd^{2+}) onto this polymer nanocomposite was important for purification, environmental and economic points of channel. The main advantages of adsorption are its simplicity, selectivity, efficiency and the separation of trace amount of bivalent metal ions from large volumes of aqueous solutions.

2. Experimental

2.1. Chemicals and reagents

Analytical grade pyrrole, ammonium persulphate (APS), hydrochloric acid (HCl), nitric acid (HNO_3) and sulphuric acid (H_2SO_4) were purchased from Merck-India. Pyrrole monomer was purified at a temperature above the boiling point of their respective monomers by distillation to remove any impurities and oligomers. MWCNT was purchased from the Applied Science and Innovation Pvt. Ltd (Pune, Maharashtra, India) (purity ≥ 95 wt%, 20–40 nm in diameter, lengths of 10–50 μm). All the chemicals and reagents used for experiments and analysis were of analytical grade.

2.2. Metal solutions

The concentration of metal ion solutions was prepared by dissolving a known quantity of PbSO_4 , $\text{NiSO}_4 \cdot 6\text{H}_2\text{O}$ and $3\text{CdSO}_4 \cdot 8\text{H}_2\text{O}$ in an appropriate amount of distilled water. The desired (100–500 mg/L) test solutions of heavy metal ions were prepared by subsequent dilutions of the stock solution. The pH of each test solution was adjusted to the required value by adding either 1 N NH_4OH or 1 N CH_3COOH .

2.3. Preparation of polymer nanocomposite adsorbent (PPy/o-MWCNT)

A PPy/o-MWCNT nanocomposite was synthesized by slightly modified procedure through in situ chemical oxidative polymerization [20]. In a typical procedure, multi-walled CNTs were oxidized via sonication in 100 mL of 1:3 (v/v) concentrated nitric acid/sulphuric acids at 60°C for 10 h. The resultant oxidized multi-walled carbon nanotubes (o-MWCNT), 1 wt% to pyrrole monomer was dispersed in 50 mL of 1 M aqueous HCl and sonicated for half an hour and poured into 0.05 mol of pyrrole in the presence of 50 mL of 1 M aqueous HCl in a 250 mL round-bottom flask and cooled down to 0–5°C. The polymerization was started by drop wise addition of the oxidant solution containing 0.05 mol of APS dissolved in 50 mL of 1 M aqueous HCl and pre-cooled at 0–5°C. The polymerization was allowed to proceed at room

temperature for 5 h with continuous stirring. The dark coloured precipitate of the polymer nanocomposite thus obtained was separated by filtration, washed with 1 M aqueous HCl followed by deionized water and finally dried in an oven at 45°C for about 24 h to remove the moisture/water (Fig. 1).

2.4. Analytical method

The attenuated total reflectance (ATR) was recorded on a Perkin Elmer, Spectrum Two spectrophotometer in the range of 4,000–400 cm^{-1} . The Raman spectrum was recorded on Bruker RFS27 operating with 1064 nm line of Nd: YAG Laser source in rock solid interferometer in the range of 100–700 cm^{-1} using liquid nitrogen-cooled germanium detector with the resolution of 4 cm^{-1} . Diffuse reflectance spectroscopy (DRS UV–vis) of the powdered sample was recorded on a Shimadzu UV-2450 spectrophotometer over the range of 190–800 nm using barium sulphate as reference. The X-ray diffraction (XRD) pattern of nanocomposites was recorded on a PANalytical X'Pert Pro X-ray diffractometer using $\text{CuK}\alpha$ as the radiation source. The diffraction was recorded in the 2θ range from 10 to 80° in steps of 0.02° with a count time of 20 s at each point. Thermogravimetric analysis was recorded using a Perkin Elmer SII (Diamond Series) model under nitrogen atmosphere in the temperature range of 30–800°C at a heating rate of 20°C/min. The morphology of the nanocomposite was examined by scanning electron microscopy (SEM) under 20 kV after gold coating using SEM-JEOL, JSM-5600 model. Cressington 108 auto sputter coater was used for coating. High-resolution transmission electron microscopic (HR-TEM) images were recorded using JEOL, JEM 2100 electron microscope operated at

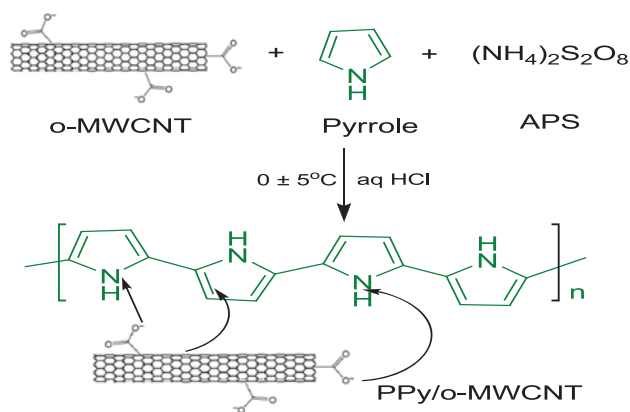


Fig. 1. Schematic representation of PPy/o-MWCNT nanocomposite adsorbent.

an accelerating voltage of 150 kV. The concentration of metal ions in the aqueous solution before and after adsorption process was determined using atomic absorption spectrophotometer (Analyst 100 Perkin Elmer) operating with an air-acetylene flame.

2.5. Adsorption studies

Adsorption equilibrium experiments were carried out in a temperature-controlled thermostatic shaker operated at 200 rpm. Followed by a systematic process, the removal of heavy metal ions from aqueous solutions by the use of PPy/o-MWCNT in a batch system was studied in the present work. The data obtained in batch studies were used to calculate the percentage removal of heavy metal ions using the following mass balance relationship [21]:

$$A(\%) = \left(\frac{C_0 - C_e}{C_0} \right) \times 100 \quad (1)$$

where “A” is the metal ions removal percentage (the amount of metal ions adsorbed per unit mass of adsorbent at time “t” (q_t , mg/g) and the amount of metal ions adsorbed per unit mass of adsorbent at equilibrium (q_e , mg/g), “ C_0 ” and “ C_e ” are the initial and equilibrium concentrations (mg/L) of metal(II) ions, respectively.

2.5.1. Effect of solution pH

The effect of solution pH on the adsorption of PPy/o-MWCNT was investigated using 20 mL of 100 mg/L metal ion solution in the pH range between 2.0 and 10.0 at 30°C. The samples were then agitated in a shaker in 200 rpm at different solutions of pH for 60 min and then filtered. The filtrates were analysed using atomic absorption spectrometer.

2.5.2. Effect of adsorbent dosage

The effect of adsorbent dosage was carried out on a different adsorbent dosage of PPy/o-MWCNT from 10 to 120 mg for 20 mL of 100 mg/L metal ion solution at pH 6 and contact time 60 min at 30°C. The samples were filtered and the filtrates were analysed as mentioned above.

2.5.3. Effect of contact time

The effect of contact time was carried out at different contact times (10–100 min) for an initial concentration of

100 mg/L metal ion solution at pH 6; the PPy/o-MWCNT dose concentration is 20 mg in 20 mL of metal ion solution into 250 mL conical flask at 30°C. The agitation time was 60 min to examine the maximum equilibrium. The mixture was then filtered and the concentration of metal ions in the filtrates was measured.

2.5.4. Effect of metal ion concentration

The effect of metal ion concentration was carried out by contacting 20 mg of PPy/o-MWCNT with 20 mL of metal ion solution of different initial concentrations (from 100 to 500 mg/L) at pH 6 in 30°C for 60 min. The samples were filtered and the filtrates were analysed as mentioned above.

2.6. Adsorption isotherms

Adsorption isotherms (30°C) were investigated at pH 6 by changing the initial concentration of metal(II) ions from 100 to 500 mg/L. The equilibrium adsorption capacity (q_e) of the adsorbent was calculated using the following equation [21]:

$$q_e = \frac{(C_0 - C_e)V}{m} \quad (2)$$

where “ m ” is the adsorbent mass (g) and “ V ” is the volume of solution (L).

2.7. Adsorption kinetics

Adsorption kinetics was calculated for the rate of metal(II) ions adsorption. The experiments were carried out for three initial concentrations (50, 75, 100 mg/L) of metal(II) ions. In a typical kinetic experiment, 20 mg of the PPy/o-MWCNT was added to 100 mL of metal(II) solution at pH 6 and stirred at 200 rpm. At a planned time interval, 5 mL of solution was collected, filtered and analysed for metal(II) concentration. The capacity of the adsorbent q_t (mg/g) at time “ t ” was obtained using the following equation [21]:

$$q_t = \frac{(C_0 - C_t)V}{m} \quad (3)$$

where “ C_t ” (mg/L) is the concentration of metal(II) ions at any time “ t ”.

2.8. Thermodynamic studies

The thermodynamic parameters of Gibbs free energy (ΔG°), enthalpy change (ΔH°) and entropy

change (ΔS°) for the adsorption processes were calculated using the Van't Hoff thermodynamic equations for the temperature range of 303–333 K [21].

$$K_c = \frac{C_{Ae}}{C_e} \quad (4)$$

$$\Delta G^\circ = -RT \ln K_c \quad (5)$$

$$\log K_c = \frac{\Delta S^\circ}{2.303R} - \frac{\Delta H^\circ}{2.303RT} \quad (6)$$

where “ K_c ” is the equilibrium constant, “ C_e ” is the equilibrium-metal ion concentration in solution (mg/L), “ C_{Ae} ” is the amount of metal ions adsorbed on the adsorbent per litre of solution at equilibrium (mg/L), “ R ” is the gas constant (8.314 J/mol K) and “ T ” is the temperature (K).

2.9. Recyclability

Recyclability of the metal(II) ions adsorbed onto PPy/o-MWCNT was studied by adsorption–desorption experiments. Initially, an adsorption test was conducted using 20 mg of the adsorbent and 20 mL of 100 mg/L metal(II) ion solution at 30°C. Thereafter, desorption experiment was performed by contacting 20 mg of metal(II)-ion loaded adsorbent with 20 mL of acidic eluent. At the end of the adsorption–desorption experiment, the adsorbent was treated with 0.2 N H_2SO_4 , HCl and CH_3COOH solution to regenerating the adsorption sites (Cl^- ion-doped state of polymer nanocomposites). To calculate the exact life cycle of the adsorbent in eliminating metal(II) ions from aqueous solution, the spent adsorbent was exposed to five successive adsorption–desorption cycles.

$$\% \text{Desorption} = \frac{\text{Amount released to solution (mg/L)}}{\text{Total adsorbed}} \times 100 \quad (7)$$

3. Results and discussion

3.1. Characterization of the adsorbent

Fig. 2 shows the ATR spectrum of PPy/o-MWCNT nanocomposite with 1 wt% of o-MWCNT wrapped in pyrrole viz in situ oxidative chemical polymerization. This spectrum shows a rich-band fingerprint region, revealing strong intensity of heteroatom. The peaks at 1,555 and 1,458 cm^{-1} are attributed to C–N, C–C asymmetric and symmetric ring-stretchings, respectively. Additionally, the strong and broad intense peak at

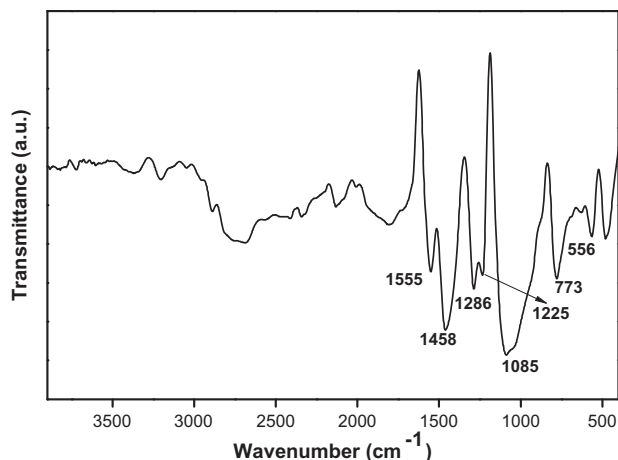


Fig. 2. ATR spectrum of PPy/o-MWCNT nanocomposite.

1,085 cm⁻¹ is attributed to C–H deformation and N–H stretching vibrations, and the sharp band at 1,286 and 1,225 cm⁻¹ demonstrates the C–H and C–N in-plane deformation vibrations, respectively [22].

The interaction between the nanotubes on the aromatic graphene basal plane was investigated by Raman spectral analysis. Raman spectrum of o-MWCNT-wrapped polypyrrole nanocomposite is shown in Fig. 3. The high intensity of the G-band peak appeared at 1,595 cm⁻¹ as compared to the low-intensity “disordered and defect” D-band peak at 1,357 cm⁻¹ demonstrates the aromatic purity of the graphene basal plane [23]. The broad peak obtained near 1,068 cm⁻¹ corresponds to the C–H in-plane deformation associated with radical cation and two small peaks near 933 and 995 cm⁻¹ are associated with the quinonoid polaronic and bipolaronic structures, respectively [24].

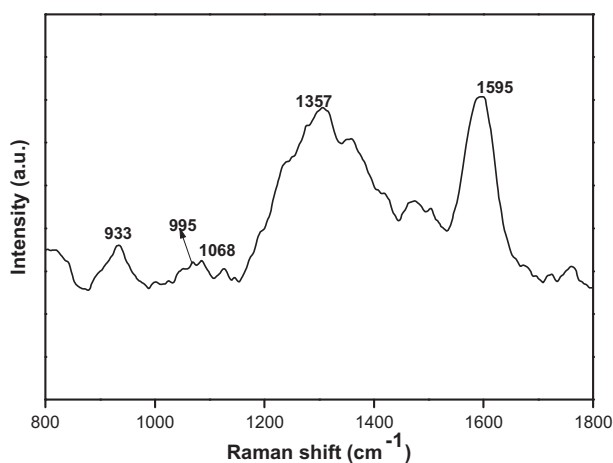


Fig. 3. Raman spectrum of PPy/o-MWCNT nanocomposite.

UV–vis spectrum of PPy/o-MWCNT nanocomposite is shown in Fig. 4. The peak at 293 nm due to π – π^* transition band is more clearly seen from the figure. Significantly, a strong band at 623 nm is also observed. MWCNT assists the polymerization in such a way that it maintains a higher conjugation length in the chain of PPy itself and there may be some coupling between the conjugation length of the PPy and MWCNT (435 nm). In addition, some functional groups such as –OH, –COOH existed on the surface and pores of the CNTs at high temperature after acid treatment could promote the adsorption of molecular chains and monomers onto the pores. Moreover, the π – π stacking between the polymer backbone and the CNTs surface may also contribute to extend the conjugation length of the polymer composite [25]. The characteristic peak of PPy/o-MWCNT nanocomposite was obtained due to the extended conjugation length of PPy chains and high degree of incorporation of CNTs which is clearly seen from Fig. 4.

Fig. 5 shows the XRD pattern of o-MWCNT-wrapped polypyrrole nanocomposite. The XRD pattern of PPy/o-MWCNT nanocomposite shows the specific characteristic peaks of catalytic particles [26] at the range of 26.05°, 44.23°, 64.59° and 77.60°, whereas the important characteristic peak of PPy ($2\theta = 26.05^\circ$) can be hardly observed and strong sharp peak at 44.23° is assigned to the interlayer spacing of the nanotube and the reflection of the carbon atoms [27]. This may be due to the adsorption and intercalation of the polymer onto the pores and galleries of the MWCNT.

The thermal stability studies show that PPy/o-MWCNT nanocomposite undergoes four stages of degradation. The TG curve of PPy/o-MWCNT is shown in Fig. 6. The initial degradation of PPy/o-MWCNT

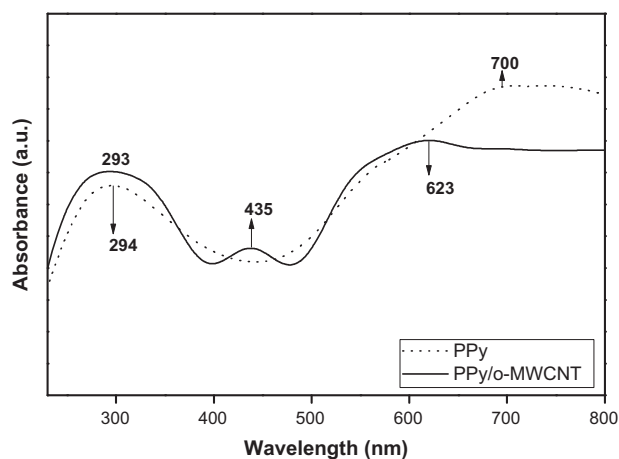


Fig. 4. DRS UV–vis analysis of PPy/o-MWCNT nanocomposite.

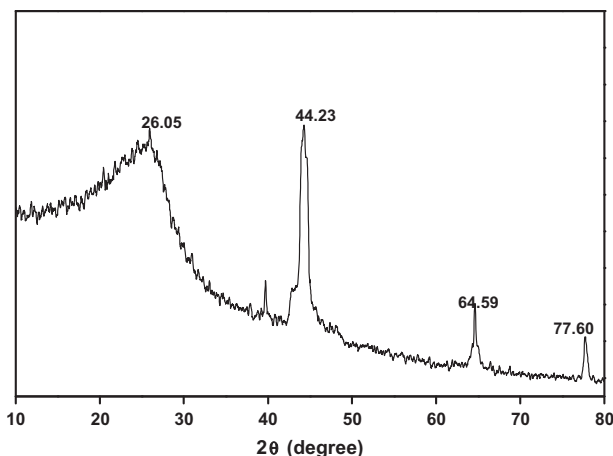


Fig. 5. XRD pattern of PPy/o-MWCNT nanocomposite.

composite is 16% at the temperature range of 30–180 °C which corresponds to the loss of moisture, volatile organic solvents and the adsorbed HCl. The second stage of elimination occurs at the temperature range of 180–320 °C with a weight loss of 14% which is probably caused by the elimination of low-molecular weight oligomers and undoped materials. Further, mild and steady degradation occurred up to 585 °C as the third degradation step. The final stage of elimination occurs between 585 and 800 °C, in which 25% mass residue is obtained [28].

The SEM images of raw Pb^{2+} , Ni^{2+} and Cd^{2+} -adsorbed polymer nanocomposite adsorbent are shown in Fig. 7. As can be seen from Fig. 7(a), the surface texture of the PPy/o-MWCNT nanocomposite is irregular (asymmetric surface), porous and has an adequate morphology for metal ion adsorption onto the surface of the polymer nanocomposite.

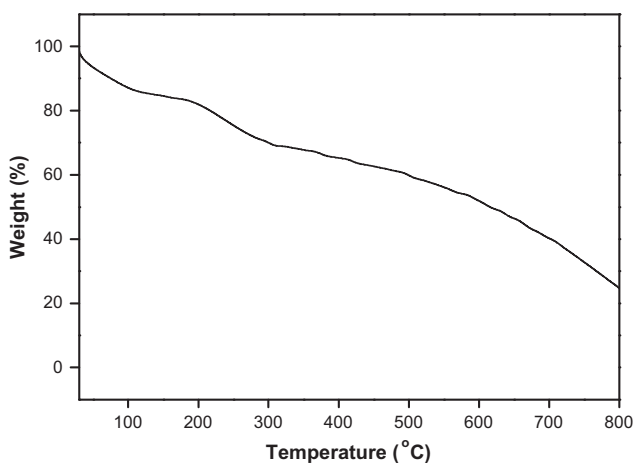


Fig. 6. TG Analysis of PPy/o-MWCNT nanocomposite.

The EDX analysis carried out confirms the adsorption of metal ions onto the adsorbent-based energy dispersion peaks obtained for the corresponding heavy metal ions. The EDX spectrum of PPy/o-MWCNT nanocomposite and the metal ion-adsorbed nanocomposite is shown in Fig. 8. Before adsorption, the EDX analysis of polymer nanocomposite shows the peak corresponding to the C, O and N atoms (Fig. 8(a)). After the metal ion adsorption, the strong peaks appear in the EDX spectrum corresponding to the obtained heavy metal ions (Fig. 8 with respect to (b)–(d)). Thus, the EDX analysis confirms the trapping of metal ions onto the polymer nanocomposite adsorbent surface. In addition to the heavy metals, such as Pb^{2+} , Ni^{2+} and Cd^{2+} ions, the new peaks corresponding to C, S and N atoms are also present. This reveals that Pb^{2+} , Ni^{2+} and Cd^{2+} ions are attached with the chelating groups such as nitro, sulpho and ether linkage in the formation of coordinate bonds.

The surface area and structural morphologies of functionalized MWCNT-wrapped polymer nanocomposite adsorbent are examined through TEM. Fig. 9(a) shows the clear images of the functionalized MWCNT well wrapped with polymer matrix. Selected area electron diffraction pattern (SAED) further confirms the metal-loaded crystalline structure of tubular MWCNT polymer nanocomposite which is shown in Fig. 9(d). Fig. 9(b) represents Pb^{2+} -loaded adsorbent, (c) represents the SAED pattern of raw polymer nanocomposite and (d) represents the SAED pattern of Pb^{2+} -loaded polymer nanocomposite adsorbent.

3.2. Effect of solution pH on metal ion adsorption

The effect of pH on heavy metal ions such as Pb^{2+} , Ni^{2+} and Cd^{2+} adsorption rates is shown in Fig. 10. The adsorption is high at pH 6 and adsorption decreases as the pH solution increases or decreases further. The maximum removal efficiencies of Pb^{2+} , Ni^{2+} and Cd^{2+} ions are 83.73, 82.68 and 81.40 mg/g, respectively. When at pH 6, the functional groups present in the adsorbent are deprotonated and their metal binding capacity increases. Hence, an optimal pH value of 6 is fixed for further adsorption experiments.

3.3. Effect of adsorbent dosage

The adsorption efficiency for Pb^{2+} , Ni^{2+} and Cd^{2+} ions as a function of adsorbent dosage is investigated. Fig. 11 shows that the adsorption increases with an increase in the dose of PPy/o-MWCNT. This could be due to the presence of o-MWCNT having large

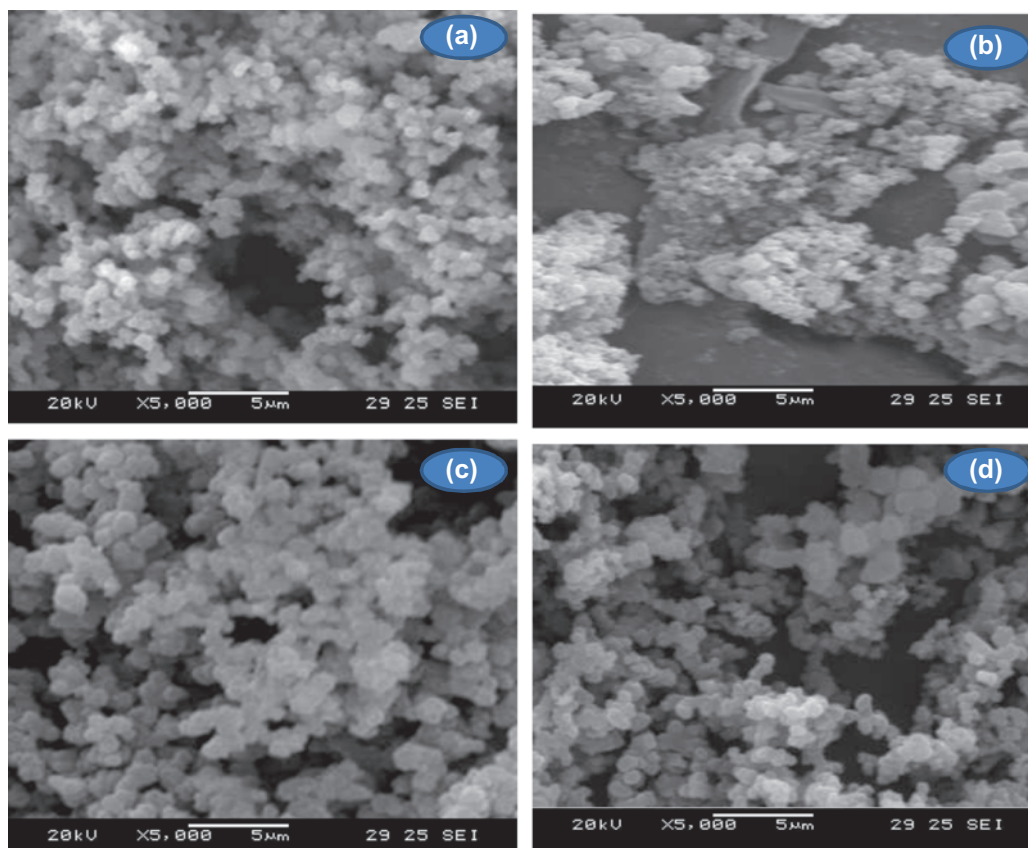


Fig. 7. Comparison of raw- and metal-loaded SEM images of PPy/o-MWCNT adsorbent. (a) SEM micrographs PPy/o-MWCNT adsorbent; (b) SEM micrographs of Pb^{2+} adsorbed PPy/o-MWCNT; (c) Ni^{2+} adsorbed PPy/o-MWCNT and (d) Cd^{2+} adsorbed PPy/o-MWCNT.

number of active sites such as oxygen and carbonyl groups and also owing to the increase in the porous nature of the composite surface [29,30]. Thus, the adsorbent at higher concentration will have a porous surface and active binding sites. The PPy/o-MWCNT adsorbent dose for Pb^{2+} , Ni^{2+} and Cd^{2+} ions from 20 to 100 mg resulted in the maximum adsorption capacity that occurs at 60 mg/g of Pb^{2+} , Ni^{2+} and Cd^{2+} for 82.27, 79.40 and 77.15%, respectively.

3.4. Effect of contact time

Fig. 12 shows the effect of contact time on the adsorption of Pb^{2+} , Ni^{2+} and Cd^{2+} ions onto PPy/o-MWCNT. The adsorption efficiency of Pb^{2+} , Ni^{2+} and Cd^{2+} ions increased considerably with an increase in the contact time up to 60 min and then, it becomes almost constant. For evidence, at 60 min, the adsorption efficiency was 83.39 mg/g, 82.71 mg/g and 81.20 mg/g for Pb^{2+} , Ni^{2+} and Cd^{2+} ions, respectively.

3.5. Effect of metal ion concentration

The removal of metal ions, such as Pb^{2+} , Ni^{2+} and Cd^{2+} , at different metal ion concentrations (100–500 mg/L) using PPy/o-MWCNT is present in Fig. 13. Adsorption capacity is gradually increased when the initial metal ion concentration increased from 100 to 500 mg/L. This is mainly due to the availability of the active sites on the adsorbent. This study gives the detail about increasing the adsorption capacity with an increase in the concentration of the metal ions; linearly, no saturation point is noticed.

The adsorption equilibrium experiment is performed and a plot for metal ions adsorbed onto the adsorbent (q_e , mg/g) against the equilibrium concentration of metal ions (C_e , mg/L) in solution at 30°C was made. Among several models available to describe adsorption isotherms, the most widely used adsorption isotherm models are the Langmuir, Freundlich and Redlich–Peterson [21].

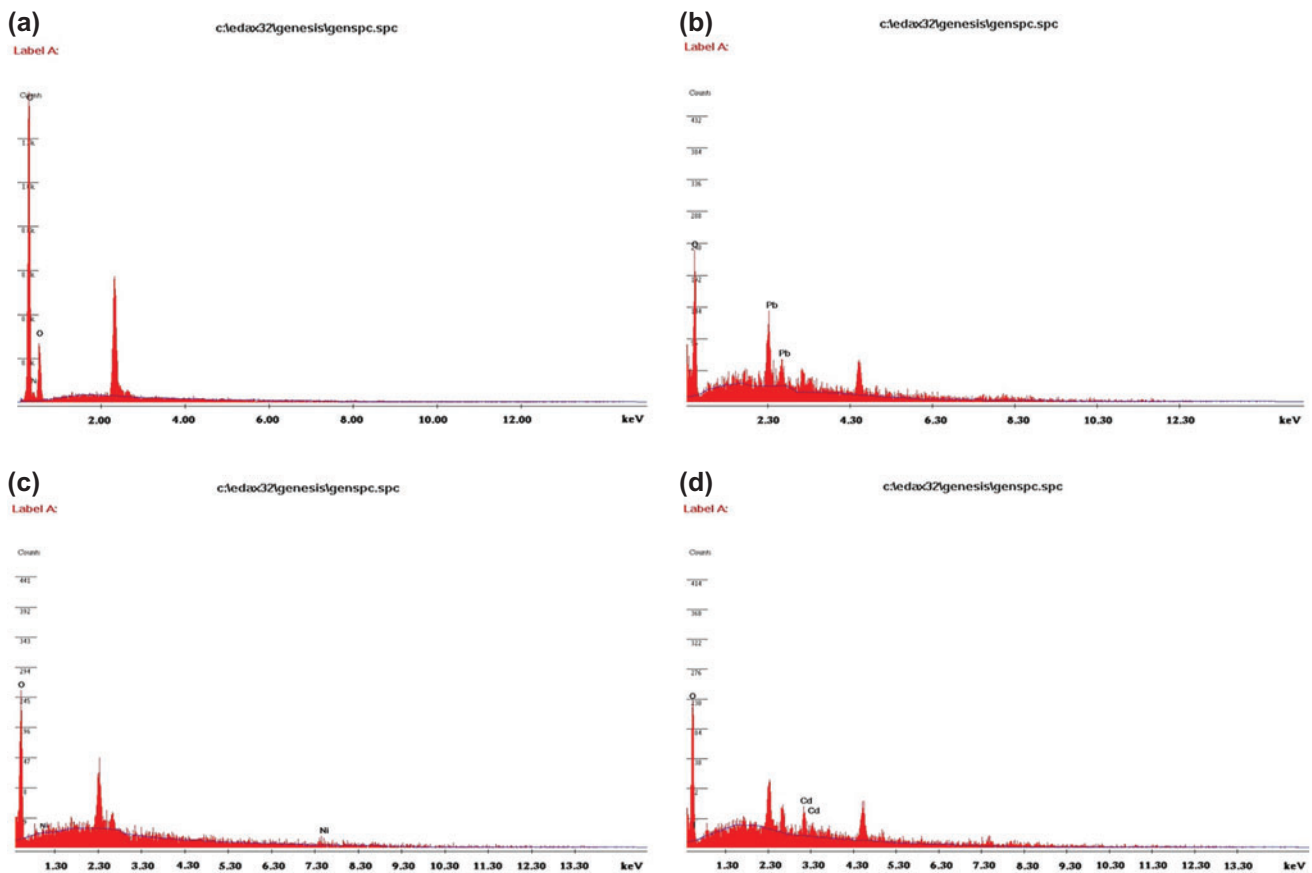


Fig. 8. Comparison of raw- and metal-loaded EDX spectrum of PPy/o-MWCNT adsorbent. (a) EDX spectrum PPy/o-MWCNT; (b) EDX spectrum of Pb^{2+} adsorbed PPy/o-MWCNT; (c) Ni^{2+} adsorbed PPy/o-MWCNT; (d) Cd^{2+} adsorbed PPy/o-MWCNT.

3.5.1. Langmuir adsorption isotherm

The Langmuir treatment is based on the assumptions that the maximum adsorption corresponds to a saturated monolayer of solute molecules on the adsorbent surface. Since, the energy of adsorption is constant and that there is no transmigration of the adsorbate on the plane of the surface. The non-linear form is represented by:

$$q_e = \frac{q_m K_L C_e}{1 + K_L C_e} \quad (8)$$

where “ q_e ” is the amount of metal adsorbed (mg/g) and “ C_e ” is the equilibrium concentration of the solution (mg/L). “ q_m ” and “ K_L ” are the Langmuir constants indicating the adsorption capacity and energy, respectively.

3.5.2. Freundlich adsorption isotherm

The Freundlich isotherm is an empirical equation and can be employed to describe the heterogeneous systems. This isotherm is derived from the assumption that the adsorption sites are distributed exponentially with respect to the heat of adsorption. It also assumes that the stronger adsorption sites are occupied first and the binding strength decreases with an increase in the binding site occupation. The non-linear form is expressed as follows:

$$q_e = K_F C_e^{1/n} \quad (9)$$

where “ K_F ” is the Freundlich constant ((mg/g) (L mg) $^{1/n}$) related to the bonding energy. “ $1/n$ ” is the heterogeneity factor and “ n ” (g/L) is a measure of the deviation from the linearity of adsorption.

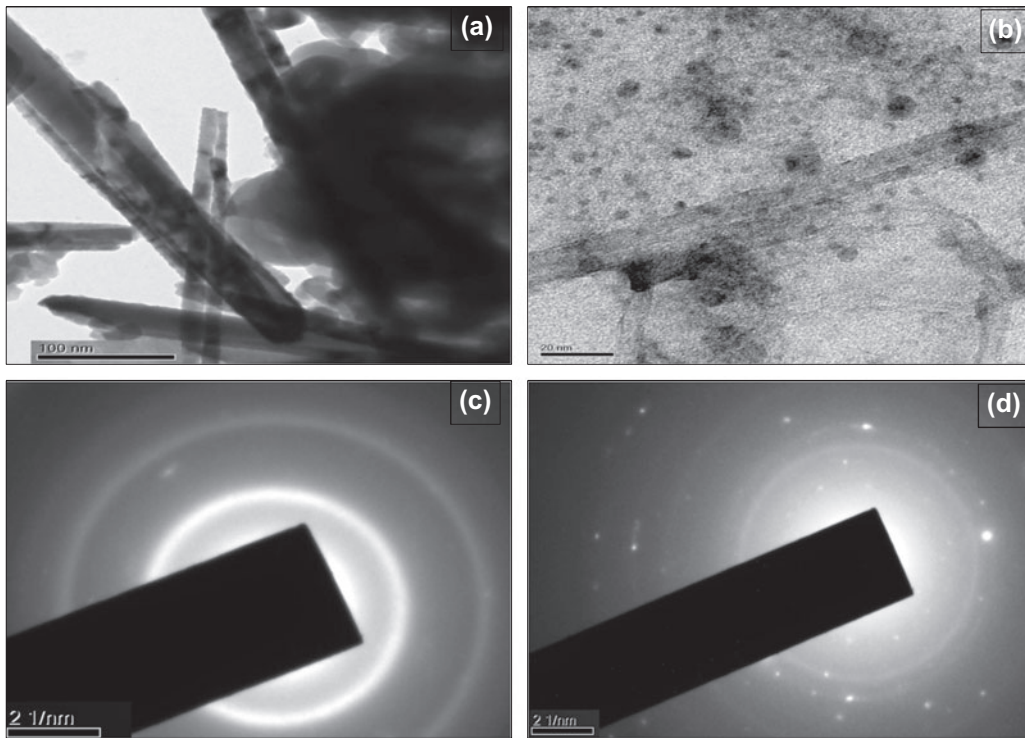


Fig. 9. Comparison TEM images of raw (a) and metal loaded (b) PPy/o-MWCNT adsorbent and SAED Pattern of raw (c) and metal loaded (d) PPy/o-MWCNT adsorbent.

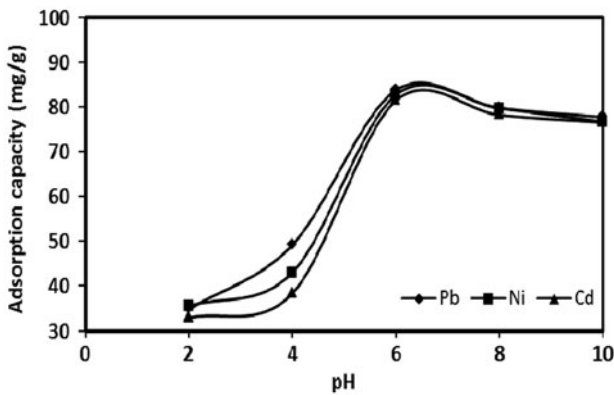


Fig. 10. Effect of the solution pH onto metal ion removal by PPy/o-MWCNT adsorbent.

Notes: Initial metal ion concentration = 100 mg/L, dose = 20 mg/L, time = 60 min and temperature = 30°C.

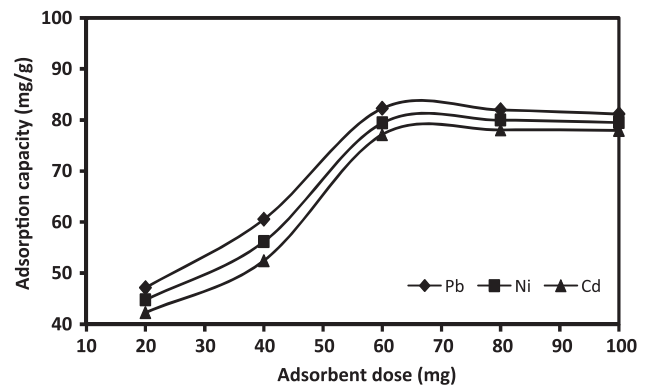


Fig. 11. Effect of the adsorbent dose onto metal ion removal by PPy/o-MWCNT adsorbent.

Notes: Initial metal ion concentration = 100 mg/L, time = 60 min, pH 6.0 and temperature = 30°C.

3.5.3. Redlich–Peterson adsorption isotherm

Redlich–Peterson isotherm is a hybrid isotherm featuring both Langmuir and Freundlich models which incorporate three parameters into an empirical equation and can be applied either in homogeneous or heterogeneous system due to its versatility. The equation is given as:

$$q_e = \frac{C_e}{1 + C_e^\beta} \quad (10)$$

where “ q_e ” is the amount of adsorbate in the adsorbent at equilibrium (mg/g), “ C_e ” is the equilibrium concentration (mg/L) and “ β ” is the exponent which lies between 0 and 1.

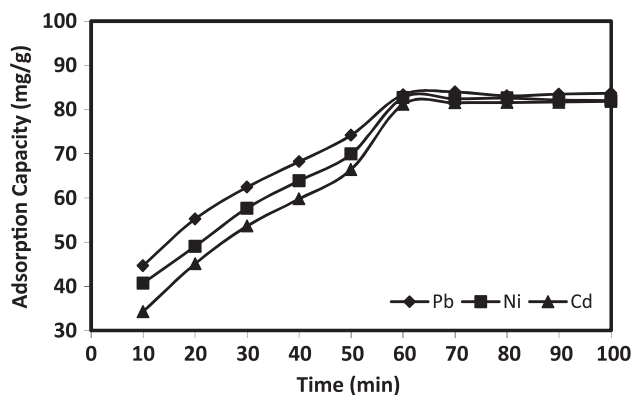


Fig. 12. Effect of the contact time onto metal ion removal by PPy/o-MWCNT adsorbent.

Notes: Initial metal ion concentration = 100 mg/L, dose = 60 mg/L, pH 6.0 and temperature = 30°C.

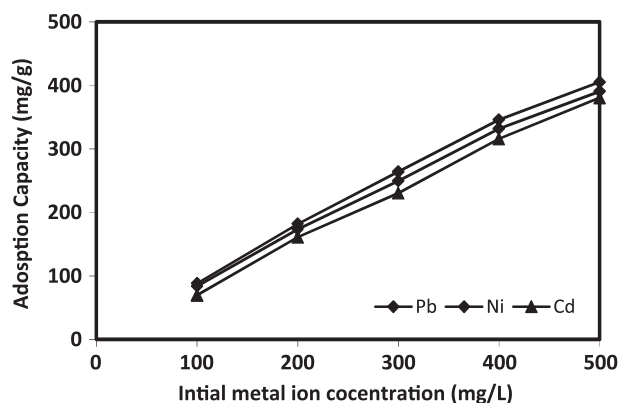


Fig. 13. Effect of initial metal ion concentrations onto metal ion removal by PPy/o-MWCNT adsorbent.

Notes: Dose = 60 mg/L, pH 6.0, time = 60 min and temperature = 30°C.

The graphical representations of these models are shown in Fig. 14. The experimental data obtained from the effect of initial concentration of the metal ions onto the surface of the PPy/o-MWCNT adsorbent are fitted into the two-parameter isotherm models using MATLAB 9.1. The Langmuir constants " q_m " (mg/g) and " K_L " (L/mg) with the " R^2 " values are calculated from the plot of " q_e " vs. " C_e " at 30°C and are listed in Table 3 (for PPy/o-MWCNT).

The Langmuir (value of R^2) and Freundlich constants " K_F " ((mg/g) (L/mg)^(1/n)) and " n " values with the " R^2 " values are estimated from the plot of " q_e " vs. " C_e " at 30°C and are listed in Table 1. The " n " values for Pb²⁺, Ni²⁺ and Cd²⁺ ions are found to be 1.81, 1.89 and 1.93, respectively, with PPy/o-MWCNT adsorbent. The value of n lies between 1 and 10 in all the

cases and this indicates that apart from chemical adsorption, adsorption also takes place through physical process [31].

The values of β for the adsorption of Pb²⁺, Ni²⁺ and Cd²⁺ onto PPy/o-MWCNT adsorbent are 0.99, 0.96 and 0.97, respectively, indicating that the Langmuir form is more applicable. Based on the R^2 values, the order of best fit for adsorption isotherms studied for each metal ion with corresponding adsorbent is presented. It could be also seen that the β value of the Redlich–Peterson isotherm was approaching 1, which means that the experimental data fit well with Langmuir model rather than Freundlich model. The result predicts the homogeneity of the adsorption sites and more likely the monolayer coverage of adsorbent surface by the Pb²⁺, Ni²⁺ and Cd²⁺ ions. The results also indicate that all the adsorption sites on the adsorbent are energetically identical.

3.6. Adsorption kinetics

Pseudo-first-order, pseudo-second-order and Elovich kinetic models were used to test the experimental data obtained from the effect of contact time and thus explain the adsorption kinetic process [21].

3.6.1. Pseudo-first-order kinetic model

Pseudo-first-order equation is the most important kinetics equation and used only for the rapid initial phase. The linearized form of the model is generally expressed as follows:

$$\log(q_e - q_t) = \log q_e - \frac{k_{ad}}{2.303} t \quad (11)$$

where " q_t " is the adsorption capacity at time " t " (mg/g) and " k_{ad} " (min⁻¹) is the rate constant of the pseudo-first-order adsorption, applied to the present study of Pb²⁺, Ni²⁺ and Cd²⁺ ion adsorption onto PPy/o-MWCNT.

The values of " q_e " and " k_{ad} " are calculated from the slope and intercept of the line obtained by the plot of $\log(q_e - q_t)$ vs. t . Fig. 15 shows the pseudo-first-order kinetic plots for the PPy/o-MWCNT nanocomposite adsorbent. Table 2 shows that the correlation coefficient (R^2) for the pseudo-first-order kinetic model is low. Moreover, a large difference of equilibrium adsorption capacity (q_e) between the experiment and calculation was observed, indicating a poor pseudo-first-order fit to the experimental data.

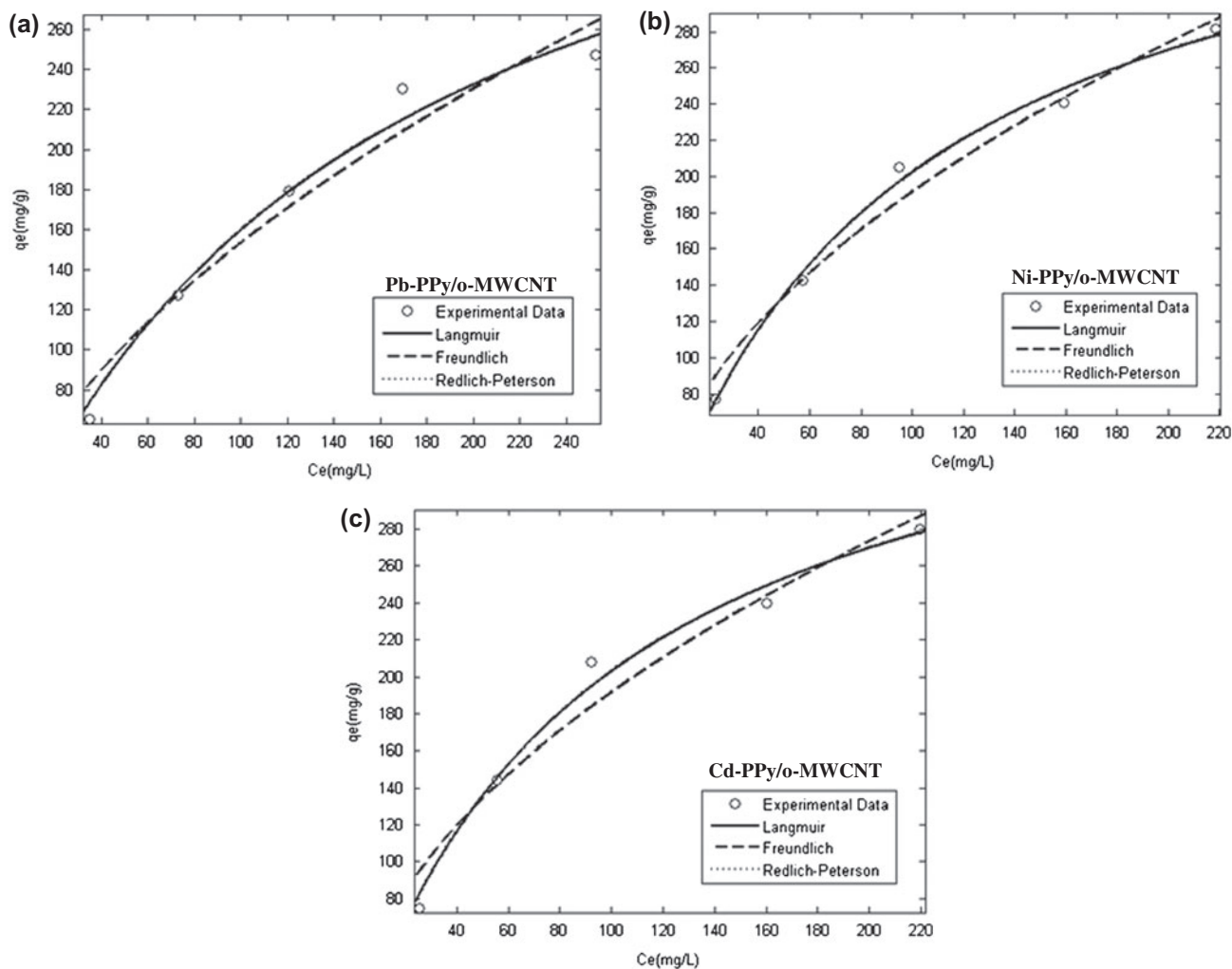


Fig. 14. Non-linear adsorption isotherm for (a) Pb^{2+} ; (b) Ni^{2+} and (c) Cd^{2+} ions onto PPy/o-MWCNT adsorbent.

Table 1
Adsorption isotherm constants for the removal of metal ions by PPy/o-MWCNT adsorbent

Isotherm model	Pb(II)		Ni(II)		Cd(II)	
	Parameter	R^2	Parameter	R^2	Parameter	R^2
Langmuir	$q_m = 408.2$ $K_L = 0.00723$	0.9483	$q_m = 409.4$ $K_L = 0.0094$	0.9876	$q_m = 392$ $K_L = 0.0094$	0.9870
Freundlich	$K_F = 12.88$ $n = 1.81$	0.9473	$K_F = 16.62$ $n = 1.89$	0.9688	$K_F = 16.61$ $n = 1.93$	0.9592
Redlich–Peterson	$K_R = 2.955$ $\alpha_R = 0.0072$ $\beta = 0.99$	0.9843	$K_R = 3.88$ $\alpha_R = 0.0094$ $\beta = 0.96$	0.9876	$K_R = 3.713$ $\alpha_R = 0.0094$ $\beta = 0.97$	0.9870

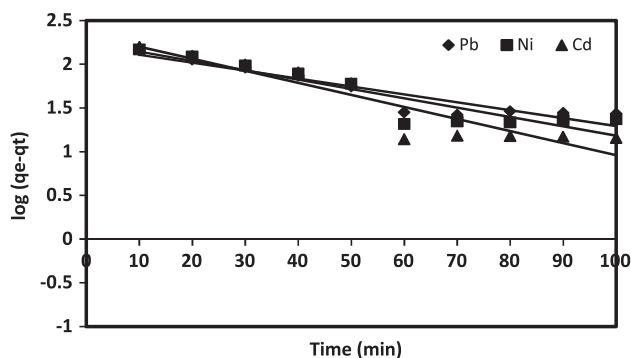


Fig. 15. Pseudo-first-order kinetic plots for the adsorption of Pb^{2+} , Ni^{2+} and Cd^{2+} ions onto PPy/o-MWCNT.

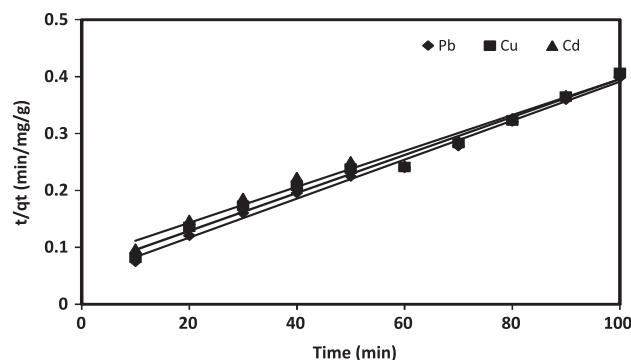


Fig. 16. Pseudo-second-order kinetic plots for the adsorption of Pb^{2+} , Ni^{2+} and Cd^{2+} ions onto PPy/o-MWCNT.

3.6.2. Pseudo-second-order kinetic model

The kinetics of the adsorption process may also be described by the pseudo-second-order rate equation. The linearized form of the equation is expressed as:

$$\frac{t}{q_t} = \frac{1}{k_2 q_e^2} + \frac{1}{q_e} t \quad (12)$$

where " k_2 " (g/mg/min) is the pseudo-second-order rate constant. The plots of " t/q_t " vs. " t " give a straight line; and the rate constant (k_2), the equilibrium adsorption capacity (q_e) and correlation coefficient (R^2) values are determined from the slopes and intercepts, respectively. At the studied contact time, straight lines with extremely high correlation coefficients ($R^2 = 0.9$) were obtained from Fig. 16 and presented in Table 2. Since, the calculated " q_e " value also agrees with the experimental data in the case of pseudo-second-order kinetic. These obtained results suggest us that the

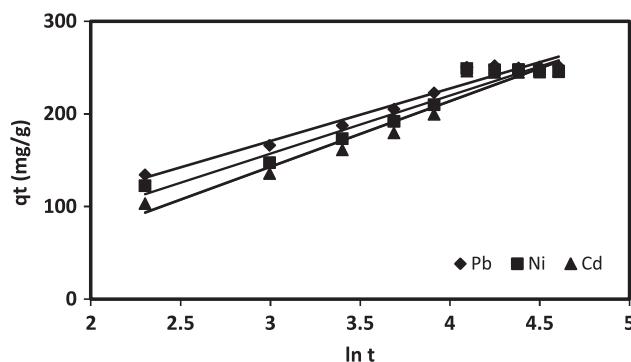


Fig. 17. Elovich kinetic model plots for the adsorption of Pb^{2+} , Ni^{2+} and Cd^{2+} ions onto PPy/o-MWCNT.

adsorption data are well fitted with the pseudo-second-order kinetics and support the statement that the rate-limiting step of Pb^{2+} , Ni^{2+} and Cd^{2+} ions onto PPy/o-MWCNT may be due to the chemisorption process.

Table 2

Kinetic parameters for the adsorption of metal ions onto PPy/o-MWCNT

Kinetic models	Parameter	Pb(II)	Ni(II)	Cd(II)
Pseudo-first-order equation	k_{ad} (min^{-1})	0.0207	0.0230	0.0299
	$q_{e,cal}$ (mg/g)	156.6	177.8	217.7
	R^2	0.8790	0.8470	0.8590
Pseudo-second-order equation	k (g/mg/min)	1.87×10^{-4}	1.45×10^{-4}	1.12×10^{-4}
	$q_{e,cal}$ (mg/g)	333.33	305.10	299.6
	h (mg/g/min)	20.83	16.12	12.5
	$q_{e,expt.}$ (mg/g)	278.03	269.47	259.84
	R^2	0.9930	0.9850	0.9770
	R^2	0.9602	0.9400	0.9437
Elovich kinetic equation	α (mg/g min)	57.15	38.46	26.80
	β (g/mg)	0.0176	0.0159	0.0140
	R^2	0.9602	0.9400	0.9437

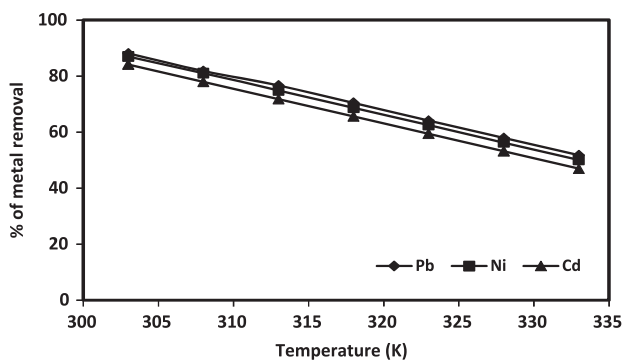


Fig. 18. Effect of temperature onto metal ions removal by PPy/o-MWCNT adsorbent.

Notes: Initial metal ion concentration = 100 mg/L, dose = 60 mg/L, time = 60 min and pH 6.0.

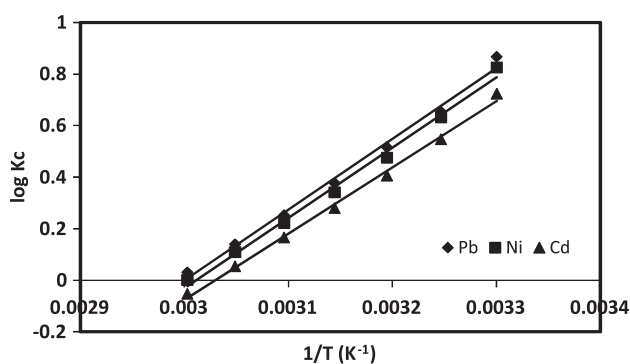


Fig. 19. Thermodynamic plots for the adsorption of metal ions onto PPy/o-MWCNT adsorbent.

3.6.3. Elovich kinetic model

The Elovich kinetic model can be expressed as:

$$q_t = \frac{1}{\beta} \ln(\alpha\beta) + \frac{1}{\beta} \ln t \tag{13}$$

where “ α ” is the initial adsorption rate in mg/(g min) and “ β ” (g/mg) is the desorption constant related to the extent of the surface coverage and activation

energy for chemisorption. The Elovich coefficient could be computed from the plot of “ q_t ” vs. $\ln t$. Pb²⁺, Ni²⁺ and Cd²⁺ ions-adsorption kinetics onto PPy/o-MWCNT were also tested with the Elovich kinetic model by plotting “ q_t ” vs. $\ln t$ obtained from Fig. 17. The recorded “ R^2 ” value is low and is represented in Table 2, which indicates the experimental data of the Elovich kinetic model and the metal ions removal using PPy/o-MWCNT under study cannot be described using this model.

3.7. Thermodynamic kinetics

Thermodynamic parameters associated with the adsorption process viz., Gibbs free energy change (ΔG), enthalpy changes (ΔH) and entropy change (ΔS) are evaluated by the Eqs. (4), (5) and (7). It has been calculated in order to evaluate the feasibility of the adsorption process. Fig. 18 indicates the percentage removal with respect to various temperatures (303–333 K). The values of ΔH° and ΔS° were determined from the slope and the intercept from the plot of $\log K_c$ vs. “ $1/T$ ” (Fig. 19) of PPy/o-MWCNT adsorbent and the thermodynamic properties are listed in Table 3.

With an increase in the temperature, negative values are obtained for the change in Gibbs free energy (ΔG) which reveals the spontaneity of the adsorption process. The negative value of ΔH confirms that energy is absorbed as the adsorption proceeds; therefore, the sorption reaction is exothermic. The change in entropy ΔS° can be used to describe the randomness involved at the adsorbent-solution interface during the adsorption of metal ions.

3.8. Recyclability of adsorbent

The regeneration of PPy/o-MWCNT was examined for feasibility considerations (Fig. 20). In order to remove the previously adsorbed Pb²⁺, Ni²⁺ and Cd²⁺ ions, the PPy/o-MWCNT is treated with an acidic solution, namely 0.2 N HCl, H₂SO₄ and CH₃COOH. The maximum recovery of 94% was obtained for 0.2 N

Table 3
Thermodynamic parameters for the adsorption of metal ions onto PPy/o-MWCNT adsorbent

PPy/o-MWCNT	ΔH° (kJ/mol)	ΔS° (J/mol/K)	ΔG° (kJ/mol)						
			303 K	308 K	313 K	318 K	323 K	328 K	333 K
Lead	-52.55	-157.67	-5.02	-3.85	-3.09	-2.29	-1.55	-0.87	-0.19
Nickel	-52.13	-156.98	-4.78	-3.71	-2.84	-2.07	-1.36	-0.68	-0.003
Cadmium	-49.18	-149.02	-4.19	-3.22	-2.42	-1.70	-1.02	-0.33	-0.34

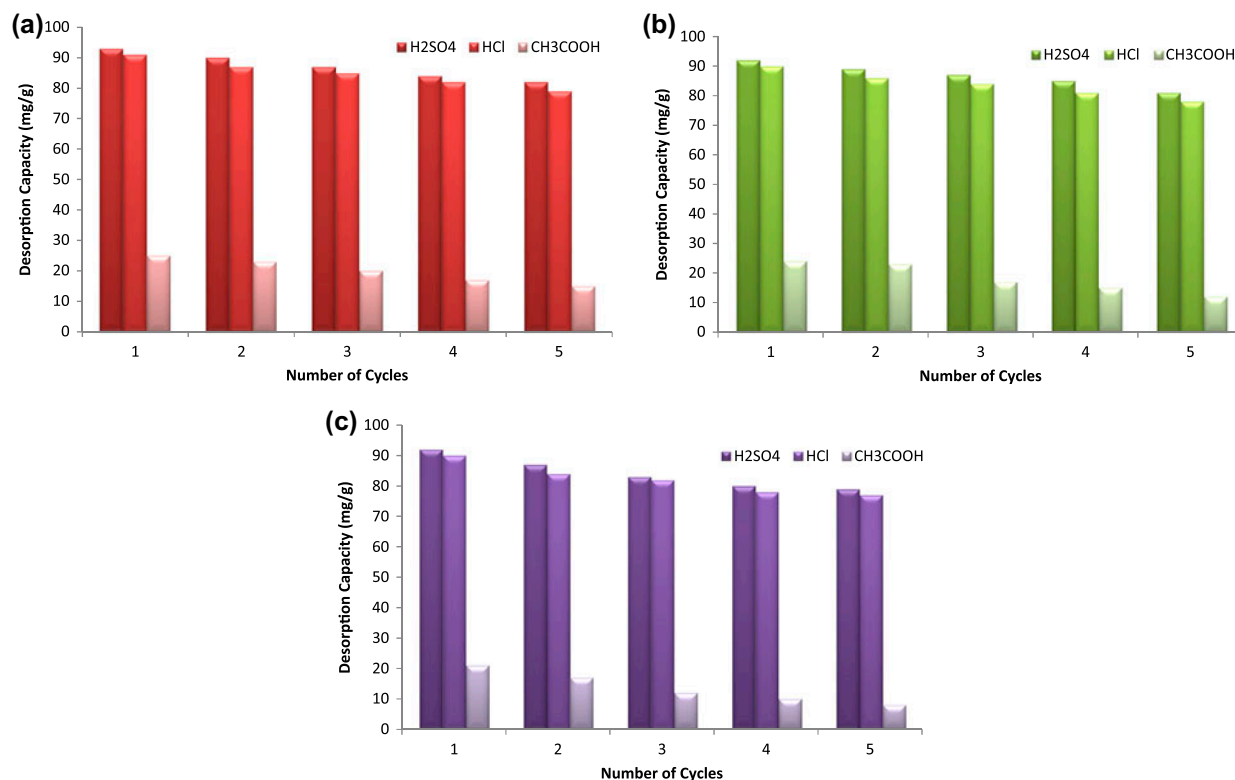


Fig. 20. Desorption studies of (a) Pb(II); (b) Ni(II) and (c) Cd(II) ions onto PPy/o-MWCNT adsorbent.

H₂SO₄ eluent and 84% was obtained for 0.2 N HCl eluent. The percentage of recovery was very low for 0.2 N CH₃COOH due to the less acidic nature when compared to others. However, it was found that the regenerated PPy/o-MWCNT could be reused for the removal of Pb²⁺, Ni²⁺ and Cd²⁺ ions without considerable loss of efficiency, even after more recycling process.

4. Conclusion

We have demonstrated the introduction of PPy/o-MWCNT nanocomposite as an adsorbent and as a strategy for functionalizing pore surfaces of CNTs. The synthesized adsorbent was confirmed with significant instrument techniques. Also we have examined all adsorption parameters such as pH, adsorbent dosage, metal ion concentration and contact time for PPy/o-MWCNT adsorbent. The isotherm data have been analysed using Langmuir, Freundlich and Redlich–Peterson isotherms. The characteristic parameters for each isotherms and related correlation coefficients have been determined using MATLAB 9. The pseudo-second-order equation provides the best correlation coefficient and agrees between the calcu-

lated “ q_e ” values and the experimental data, rather than other kinetic equations. The o-MWCNT-wrapped PPy nanocomposite provides larger binding sites and porous surface material to give enhanced adsorption capacity for Pb²⁺, Ni²⁺ and Cd²⁺ ions and very suitable, easily producible, high selectivity, high thermal stability and a great possibility of a filter for other heavy metal ions.

Supplementary material

The supplementary material for this paper is available online at <http://dx.doi.org/10.1080/19443994.2015.1081629>.

Acknowledgements

The research upon which this paper is based was supported by a grant from DST-FIST, UGC New Delhi, Govt. of India is acknowledged for their assistance with experimental design and analysis. The authors would also like to acknowledge financial support from the Anna Centenary Research Fellowship, Anna University, Chennai, Government of Tamil Nadu, India.

References

- [1] D. Mohan, K.P. Singh, Single- and multi-component adsorption of cadmium and zinc using activated carbon derived from bagasse—An agricultural waste, *Water Res.* 36 (2002) 2304–2318.
- [2] T.K. Sen, S.P. Mahajan, K.C. Khilar, Adsorption of Cu^{2+} and Ni^{2+} on iron oxide and kaolin and its importance on Ni^{2+} transport in porous media, *Colloids Surf., A* 211 (2002) 91–102.
- [3] A.B. Pérez-Marín, V.M. Zapata, J.F. Ortuño, M. Aguilar, J. Sáez, M. Lloréns, Removal of cadmium from aqueous solutions by adsorption onto orange waste, *J. Hazard. Mater.* 139 (2007) 122–131.
- [4] M.E. Mahmoud, M.M. Osman, O.F. Hafez, A.H. Hegazi, E. Elmelegy, Removal and preconcentration of lead(II) and other heavy metals from water by alumina adsorbents developed by surface-adsorbed-dithione, *Desalination* 251 (2010) 123–130.
- [5] Z. Zulfadhly, M.D. Mashitah, S. Bhatia, Heavy metals removal in fixed-bed column by the macro fungus *Pyrenopeziza sanguineus*, *Environ. Pollut.* 112 (2001) 463–470.
- [6] P.K. Jal, S. Patel, B.K. Mishra, Chemical modification of silica surface by immobilization of functional groups for extractive concentration of metal ions, *Talanta* 62 (2004) 1001–1028.
- [7] M. Sekar, V. Sakthi, S. Rengaraj, Kinetics equilibrium adsorption study of lead(II) onto activated carbon prepared from coconut shell, *J. Colloid Interface Sci.* 279 (2004) 307–313.
- [8] Y.S. Ho, G. McKay, The sorption of lead(II) ions on peat, *Water Res.* 33 (1999) 578–584.
- [9] J. Ayala, F. Blanco, P. García, P. Rodriguez, J. Sancho, Asturian fly ash as a heavy metals removal material, *Fuel* 77 (1998) 1147–1154.
- [10] Q. Li, S. Wu, G. Liu, X. Liao, X. Deng, D. Sun, Y. Hu, Y. Huang, Simultaneous biosorption of cadmium(II) and lead(II) ions by pretreated biomass of *Phanerochaete chrysosporium*, *Sep. Purif. Technol.* 34 (2004) 135–142.
- [11] B. Biskup, B. Subotic, Removal of heavy metal ions from solutions using zeolites. III. Influence of sodium ion concentration in the liquid phase on the kinetics of exchange processes between cadmium ions from solution and sodium ions from zeolite A, *Sep. Sci. Technol.* 39 (2004) 925–940.
- [12] C.V. Diniz, F.M. Doyle, V.S.T. Ciminelli, Effect of pH on the adsorption of selected heavy metal ions from concentrated chloride solutions by the chelating resin Dowex M-4195, *Sep. Sci. Technol.* 37 (2002) 3169–3185.
- [13] Y.H. Li, Z. Di, J. Ding, D. Wu, Z. Luan, Y. Zhu, Adsorption thermodynamic, kinetic and desorption studies of Pb^{2+} on carbon nanotubes, *Water Res.* 39 (2005) 605–609.
- [14] R.C. Haddon, Carbon nanotubes, *Acc. Chem. Res.* 35 (2002) 977–1113.
- [15] Y.H. Li, J. Ding, Z. Luan, Z. Di, Y. Zhu, C. Xu, D. Wu, B. Wei, Competitive adsorption of Pb^{2+} , Cu^{2+} and Cd^{2+} ions from aqueous solutions by multiwalled carbon nanotubes, *Carbon* 41 (2003) 2787–2792.
- [16] D. Shao, C. Chen, X. Wang, Application of polyaniline and multiwalled carbon nanotube magnetic composites for removal of Pb(II), *Chem. Eng. J.* 185–186 (2012) 144–150.
- [17] M. Nishizawa, T. Matsue, I. Uchida, Fabrication of a pH-sensitive microarray electrode and applicability to biosensors, *Sens. Actuators B.* 13(1–3) (1993) 53–56.
- [18] B. Saoudi, N. Jammul, M.L. Abel, M.M. Chehimi, G. Dodin, DNA adsorption onto conducting polypyrrole, *Synth. Met.* 87 (1997) 97–103.
- [19] P.A. Kumar, M. Ray, S. Chakraborty, Hexavalent chromium removal from wastewater using aniline formaldehyde condensate coated silica gel, *J. Hazard. Mater.* 143 (2007) 24–32.
- [20] S. Dhibar, S. Sahoo, C.K. Das, Fabrication of transition-metal-doped polypyrrole/multiwalled carbon nanotubes nanocomposites for supercapacitor applications, *J. Appl. Polym. Sci.* 130 (2013) 554–562.
- [21] P. Kumar, S. Ramalingam, V. Sathyaselvabala, S. Kirupha, A. Murugesan, S. Sivanesan, Removal of cadmium(II) from aqueous solution by agricultural waste cashew nut shell, *Korean J. Chem. Eng.* 29(6) (2012) 756–768.
- [22] T.M. Wu, H.L. Chang, Y.W. Lin, Synthesis and characterization of conductive polypyrrole/multiwalled carbon nanotubes composites with improved solubility and conductivity, *Compos. Sci. Technol.* 69 (2009) 639–644.
- [23] T.M. Wu, S.H. Lin, Characterization and electrical properties of polypyrrole/multiwalled carbon nanotube composites synthesized by in situ chemical oxidative polymerization, *J. Polym. Sci., Part B: Polym. Phys.* 44 (2006) 1413–1418.
- [24] G. Han, J. Yuan, G. Shi, F. Wei, Electrodeposition of polypyrrole/multiwalled carbon nanotube composite films, *Thin Solid Films* 474 (2005) 64–69.
- [25] S. Konwer, J. Maiti, S.K. Dolui, Preparation and optical/electrical/electrochemical properties of expanded graphite-filled polypyrrole nanocomposites, *Mater. Chem. Phys.* 128 (2011) 283–290.
- [26] O. Zhou, R.M. Fleming, D.W. Murphy, C.H. Chen, R.C. Haddon, A.P. Ramirez, S.H. Glarum, Defects Carbon Nanostruct., *Science* 263 (1994) 1744–1747.
- [27] V. Georgakilas, P. Dallas, D. Niarchos, N. Boukos, C. Trapalis, Polypyrrole/MWNT nanocomposites synthesized through interfacial polymerization, *Synth. Met.* 159 (2009) 632–636.
- [28] Y.K. Lee, K.J. Lee, D.S. Kim, D.J. Lee, J.Y. Kim, Polypyrrole carbon nanotube composite films synthesized through gas-phase polymerization, *Synth. Met.* 160 (2010) 814–818.
- [29] H.J. Wang, A.L. Zhou, F. Peng, H. Yu, L.F. Chen, Adsorption characteristic of acidified carbon nanotubes for heavy metal Pb(II) in aqueous solution, *Mater. Sci. Eng., A* 466 (2007) 201–206.
- [30] E. Sahmetlioglu, E. Yilmaz, E. Aktas, M. Soylak, Polypyrrole/multi-walled carbon nanotube composite for the solid phase extraction of lead(II) in water samples, *Talanta* 119 (2014) 447–451.
- [31] K.Y. Foo, B.H. Hameed, Insights into the modeling of adsorption isotherm systems, *Chem. Eng. J.* 156 (2010) 2–10.